Anatomical Correlates and Surgical Considerations for Localized Therapeutic Hypothermia Application in Cochlear Implantation Surgery

*Enrique Perez, *‡Andrea Viziano, *Zaid Al-Zaghal, *Fred F. Telischi, *Rachele Sangaletti,
†Weitao Jiang, §William Dalton Dietrich, ||Curtis King, *Michael E. Hoffer,
and *†Suhrud M. Rajguru

*Department of Otolaryngology; †Department of Biomedical Engineering, University of Miami, Miami, Florida; ‡Department of Clinical Sciences and Translational Medicine, University of Rome Tor Vergata, Rome, Italy; §Department of Neurological Surgery, The Miami Project to Cure Paralysis, University of Miami, Miami, Florida; and ||Lucent Medical Systems, Seattle, Washington

Hypothesis: Application of localized, mild therapeutic hypothermia during cochlear implantation (CI) surgery is feasible for residual hearing preservation.

Background: CI surgery often results in a loss of residual hearing. In preclinical studies, local application of controlled, mild therapeutic hypothermia has shown promising results as a hearing preservation strategy. This study investigated a suitable surgical approach to deliver local hypothermia in patients utilizing anatomical and radiologic measurements and experimental measurements from cadaveric human temporal bones.

Methods: Ten human cadaveric temporal bones were scanned with micro-computed tomography and anatomical features and measurements predicting round window (RW) visibility were characterized. For each bone, the standard facial recess and myringotomy approaches for delivery of hypothermia were developed. The St. Thomas Hospital (STH) classification was used to record degree of RW visibility with and without placement of custom hypothermia probe. Therapeutic hypothermia was delivered through both approaches and temperatures recorded at the RW, RW niche, over the lateral semicircular canal and the supero-lateral mastoid edge.

Results: The average facial recess area was $13.87 \pm 5.52 \, mm^2$. The introduction of the cooling probe through either approach did not impede visualization of the RW or cochleostomy as determined by STH grading. The average temperatures at RW using the FR approach reduced by $4.57 \pm 1.68 \,^\circ C$ for RW, while using the myringotomy approach reduced by $4.11 \pm 0.98 \,^\circ C$ for RW.

Conclusion: Local application of therapeutic hypothermia is clinically feasible both through the facial recess and myringotomy approaches without limiting optimal surgical visualization. **Key Words:** Cochlea—Cochlear implant—Electrode insertion—Hearing—Hearing loss—Neuroprosthetics—Residual hearing—Therapeutic hypothermia.

Otol Neurotol **40:**1167–1177, 2019.

Cochlear implants (CI) have become the standard worldwide treatment for severe to profound hearing loss benefitting more than half a million patients with sensorineural hearing loss (1,2). Traditional CI patients have severe to profound bilateral sensorineural hearing loss and poor speech discrimination scores. With refined diagnostics, technological improvements and considerations for recipients' quality of life, implantation criteria have broadened over the years (3,4). Today candidates include patients with single-sided deafness, and those with significant residual hearing. The latter encompasses a population with adequate thresholds in low-frequency

pure tone audiometry but poor scores on speech perception testing in best-fitted conditions. Outcomes research has demonstrated that post-implantation these individuals achieve significant improvements in speech scores. With postoperative hearing preservation, patients demonstrate significant benefits from bimodal electroacoustic stimulation (EAS) (5). The acoustic amplification in EAS devices provides a more accurate representation of real-world sounds, resulting in superior speech recognition with competing background noise, enhanced music appreciation and improvements in sound localization (6–10).

Electrode insertion can result in direct trauma to intracochlear structures including the basilar membrane, osseous spiral lamina, stria vascularis, and modiolus (11–16). Disruptions in the endocochlear potential secondary to fluid shifts and the onset of inflammatory molecular cascades following acute trauma can damage any residual hair cells (11–16). In a recent clinical trial for EAS CI, the most prevalent and significant adverse event was the loss of residual hearing affecting 44% of the study population (17). EAS CI patients have been observed to lose greater than 30 dB of residual low frequency hearing up to several months post-implantation (5,18–21).

In efforts to reduce electrode insertion trauma, soft surgery techniques and new electrode array designs have been introduced. Soft surgery techniques include minimizing vibrational trauma by employing low drill speeds, utilizing lubricating mediums (hyaluronic acid) to limit frictional forces and intracochlear contamination, slow insertion speeds, and employing electrocochleography measurements during insertion (22–26). The choice between a round window (RW) and independent cochleostomy insertion has also been a topic of debate. With advances in imaging technology, high-resolution computer tomography has also been used to better study the insertion vectors in relation to extracochlear anatomic variations and scalar dimensions (27,28). Short hybrid arrays have been introduced to avoid deep insertions that jeopardize residual hearing. Finally, dexamethasone-eluting electrodes are being investigated to complement the widely exercised practice of perioperative steroid use to minimize post-CI intracochlear inflammation (29–34).

Local application of mild, therapeutic hypothermia has been proposed in preclinical animal studies to reduce inflammation post-CI and protect hair cells and residual hearing with promising results (35,36). Neuroprotective effects of hypothermia result from a reduction in oxidative stress, suppression of excitotoxicity, and inflammation (37–39). Studies on animal models of cochlear ischemia-induced hearing loss have demonstrated that therapeutic hypothermia carries significant otoprotective effects (40,41). Previous work by our group demonstrated the feasibility of locally applying hypothermia to the inner ear during CI surgeries, both via development of a computational model and by applying a customized cooling probe device to human temporal bones (36). This approach of transient introduction of a probe to deliver hypothermia therapy carries a high translational potential

for hearing preservation surgeries. However, the addition of a probe into the already constrained anatomy of a standard facial recess approach may be a limiting factor. In clinical practice, it could be difficult to maintain optimal visualization of RW for implant insertion while maintaining adequate placement of the hypothermia probe on the promontory. The present study investigated the anatomical constraints and surgical correlates of a standard posterior tympanotomy (facial recess) and a transtympanic (myringotomy) approach in adult cadaveric temporal bones for the cooling probe placement to deliver local hypothermia in the setting of CI.

MATERIALS AND METHODS

Micro-computed Tomography

This study was exempted by the Institutional Review Board. Ten human adult cadaveric temporal bones (six left and four right), from donors with no recorded history of ear disease (four men, two women, mean age 63.4 yr) were obtained. A high-resolution microtomography scanner (SkyScan 1176, Micro Photonic Inc., Allentown, PA) was used to obtain micro-computed tomography (μCT) scans of the bones in a standardized anatomical position mimicking that of axial temporal bone scans used in clinical settings. Images were acquired with slice thickness of 34 μm and at least 500 axial slices per specimen. Image sequences for each bone were loaded into ImageJ (http://rsbweb.nih.gov/ij/) and analyzed (spatial resolution of 34 μm/pixel). Measurements were acquired to estimate overall facial recess (FR) area assuming an intact incudal buttress. Using defined landmarks such as the origin of the chorda tympani (ChT), floor of the external auditory canal (EAC), midway point between the ChT origin and EAC floor, the RW, and the bony annulus exit-point of the ChT, distances between the facial nerve (FN) and the ChT were measured (Fig. 1). Similarly, the FR height was calculated in vertical segments between axial planes depicting these landmarks. Total height was obtained with the sum of these segments. Together these measurements were used to estimate overall area of the FR. The region was separated into four zones (Fig. 2) and their respective areas summed. Additional measurements and extracted parameters followed previous work (42) to predict RW visibility during FR approach. Two measurements (EAC angle and FN location, Fig. 1D and E) were taken for each bone using the image slice where the RW was best visible. EAC angle is defined between a line tangential to the posterior EAC wall and one drawn along the axis of the cochlear basal turn (BT). FN Location is the distance between the BT axis line and the anterior-most boundary of FN.

Surgical Preparation

Following imaging, bones were thawed overnight at room temperature. FR was approached by canal wall up mastoidectomy; its boundaries (ChT, FN, and incudal buttress) were identified and preserved while maximizing bony removal, including thinning of the posterior canal wall and bone overlying the FN to simulate standard surgical steps of CI surgery. After completion of the posterior tympanotomy or facial recess and removal of any obvious bony niche overhangs, the surgeons were asked to record their judgment of RW visibility according to the St. Thomas Hospital classification (STH) (43). STH grades exposure of the RW membrane into type 1 (observed in entirety), 2a (>50% but <100% exposed), 2b (<50%) and 3
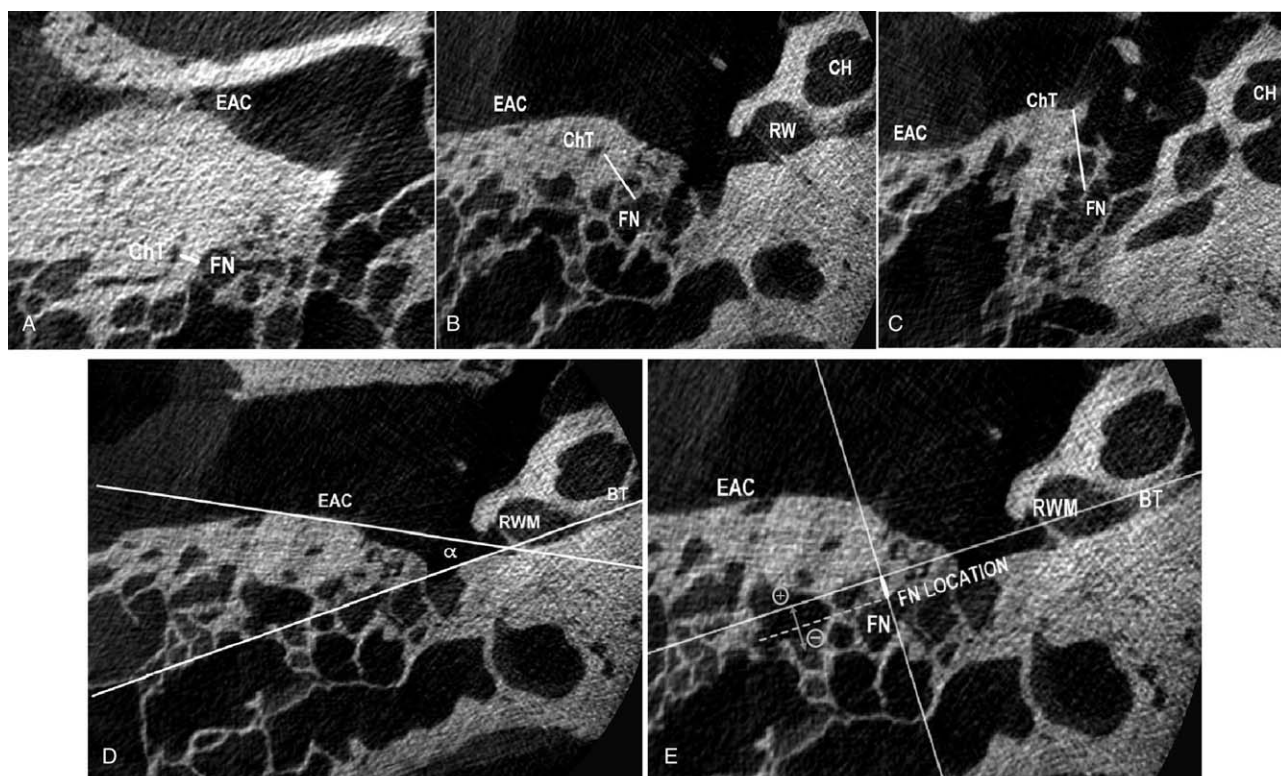
FIG. 1. *A−C*: μCT measurements depicting distances between the chorda tympani (ChT) and the facial nerve (FN) at the most inferior aspect of the external auditory canal (EAC) (*A*), at the level of the round window (RW) (*B*), and at the bridging of ChT with the tympanic ring, e.g., the image slice where ChT is last recognizable exiting its bony canal (*C*). *D*: EAC angle (*α*) between a line passing through the bony-cartilaginous junction of EAC and the tympanic ring, and a line passing through the center of the basal turn (BT) of cochlea (CH). *E*: Facial nerve (FN) Location, distance between the anterolateral edge of the FN and a line perpendicular to the BT.

(membrane not identifiable even with the best surgical effort). Promontory drilling was then conducted to create an extended RW exposure or develop an independent cochleostomy if poor initial visibility called for these maneuvers. Finally, the EAC was dissected to fully visualize the tympanic membrane, and a myringotomy was performed for transtympanic access to the promontory. To assess feasibility of CI insertion with simultaneous cochlear cooling, a second set of STH grades (STH Post-) was obtained for each bone with the cooling probe inserted through the facial recess or myringotomy.
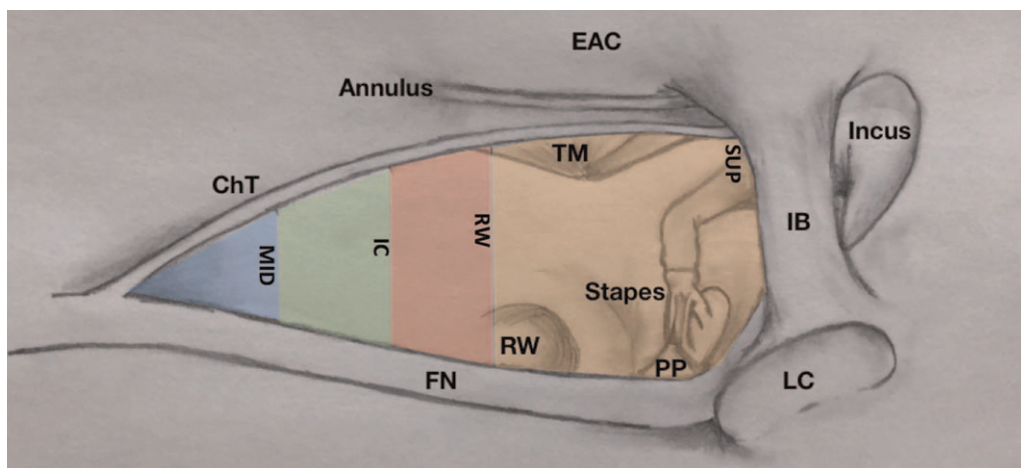
FIG. 2. Illustration depicting the approximate colored segments developed using various facial recess measurements as detailed under μCT measurements in the methods section. Areas of each segment were independently calculated and summed to estimate total facial recess area. Horizontal measurements were based on distances between the chorda tympani (ChT) and the facial nerve (FN). Vertical measurements were based on distances between defined landmarks such as origin of ChT, inferior-most border of the external auditory canal (not depicted in this illustration), round window (RW), and superior limit of the ChT as it exits the bony annulus. The shorter distances between the nerves were measured halfway between an axial plane crossing the origin of the chorda and at the inferior-most border of the EAC ("MID"). IB indicates incudal buttress; LC, lateral semicircular canal; PP, pyramidal process; TM, tympanic membrane.

Radiologic measurements of total FR area, FN location, and EAC angle were correlated with surgical visualization assessments and with results of the hypothermia experiments to determine if these factors could impact the success of cochlear hypothermia during a simulated standard CI surgery.

Hypothermia Experiments

Bones were warmed to 37 °C by submerging them in a bead bath (ThermoFisher Scientific, TSGP05, Waltham, MA) containing metallic beads (Lab Armor Beads) set to 50 °C. To maintain constant temperature during experimental measurements, bones remained submerged in the bath (Fig. 3C and D). The cooling probe is 1.6 mm in diameter and 5 mm in tip length with a 50 μM gold coating and securely connected to custom multi-lumen tubing (Fig. 3A and B, (35,36)). Using both the facial recess and the myringotomy approaches, the probe was positioned over the promontory and secured in place extra-temporally to perform the timed hypothermia experiments. Anatomical constraints and the geometry of the probe ensured that it stayed steady without additional support. As the refrigerant, temperature-controlled fluorocarbon was perfused through the tubing and probe. The RW was pierced with a Rosen needle, and the cochlea was perfused with phosphate-buffered saline warmed to 37 °C. Four microthermistors (QTI Sensing Solutions T320/E320) were placed inside the cochlea as far as it could travel (Apex), at RW annulus, over the lateral semicircular canal (LC) outer surface and over the supero-lateral edge of the mastoidectomy (M).

For both surgical approaches, a hypothermia protocol was performed three times consecutively for each bone using our custom-designed system and probe. The experimental order between approaches was randomized for each bone. When switching approaches, thermistors were left in place and only the probe was replaced. The probe target temperature reflected the temperature of the fluorocarbon within the probe lumen measured with a microthermister (Fig. 3B). This temperature was recorded along with the four sites (RW, Apex, LC, and M) over the entire procedure. During the cooling phase, the probe target temperature, controlled by the fluorocarbon temperature, was lowered every 2 minutes in the following steps: 33 to 30 to 25 to 20 to 15 to 10 to 5 °C. Following previously established protocol (35,36), the probe temperature was maintained at 5 °C for 40 minutes. Rewarming mimicked target temperature steps and timing from the cooling phase in reverse reaching 33 °C.

Statistical Analysis

The maximum change in temperature (cooling achieved) at RW, apex, LC and M measured over the duration of hypothermia protocol were compared between the two surgical approaches using Student t test. The time to achieve a change of at least 2 °C for all four locations was compared. Linear regression models were fit to test whether facial recess area, EAC angle, or FN location affected the cooling efficiency (maximum change in temperature) or rate constants (time to cool) in either surgical approaches. All statistical analysis was conducted in R (R Foundation for Statistical Computing).

RESULTS

Anatomical Measurements

The FR area in this group of temporal bones was 13.87 ± 5.52 mm^2 (mean $\pm$ s.d., range of 8.44–24.28 mm^2, Table 1). The widest horizontal distance between the FN and ChT was found at the superior landmark (SUP) where the chorda exits its bony canal adjacent to the tympanic ring. The average distance at this point was 2.86 ± 0.77 mm (2–4.3 mm). Conversely, the shorter distances between the nerves were measured halfway between an axial plane crossing the origin of the chorda and at the inferior-most border of the EAC (''MID''). The average distance at this point was 0.91 ± 0.55 mm (0.4–1.5).

Significant variability was observed in the vertical measurements in the facial recess. The widest range in distances was found in the IC/RW vertical segments, which represent the vertical distances between an axial plane depicting the inferior-most aspect of the EAC and a plane depicting the inferior-most aspect of the RW (Fig. 2). The average IC/RW vertical distance in the group of specimens was 3.99 ± 1.84 mm (0.54–5.71). Although it also demonstrated considerable variability, the RW/SUP vertical segment was the shortest with an average distance of 0.96 ± 1.2 mm (0–3.88). Several specimens demonstrated a ChT exiting its bony canal near or at the level of RW. For those with the two landmarks coinciding at the same axial plane the RW/SUP vertical distance was recorded as 0, partially explaining variability in the measurements reported (Table 1).

There was significant variability in the EAC angle: 18.75 ± 9.4 degrees (8.59–35.7 degrees). The distance between the basal turn line and the anterolateral-most aspect of the FN (FN Location) was depicted as a negative number (unfavorable) if the line fell behind the nerve edge or positive (favorable) if it was found anterior to it. Across the samples, FN Location ranged from −1.74 to 1.3 mm.

Table 2 depicts the STH classification scores for each specimen. This was first determined with bones in the appropriate surgical position having completely opened the facial recess and removed RW niche bony overhangs. Having performed the necessary drilling to better expose the RW or create an independent cochleostomy, the additional introduction of the cooling probe through either approach had no impact on cochleostomy visualization as depicted by the STH Post-rating of 1 for all the bones in Table 2. Bones requiring interventions other than removal of overhangs for better visualization (1, 8, 9, and 10) on average had smaller EAC angles (13.1 degrees) than those not requiring intervention (22.6 degrees) but the difference did not achieve statistical significance. When analyzing the calculated total FR area between these two groups there was no significant difference, with the intervention group averaging an area of 14.1 mm^2 and the non-intervention group averaging an area of 13.9 mm^2. The basal turn line appeared favorable in relation to the location of the FN in 50 and 67% of the specimens for the intervention and non-intervention groups, respectively.

Therapeutic Hypothermia and Temperature Measurements

Detailed temperature profiles over time, in three consecutive repeated hypothermia protocols for one sample,
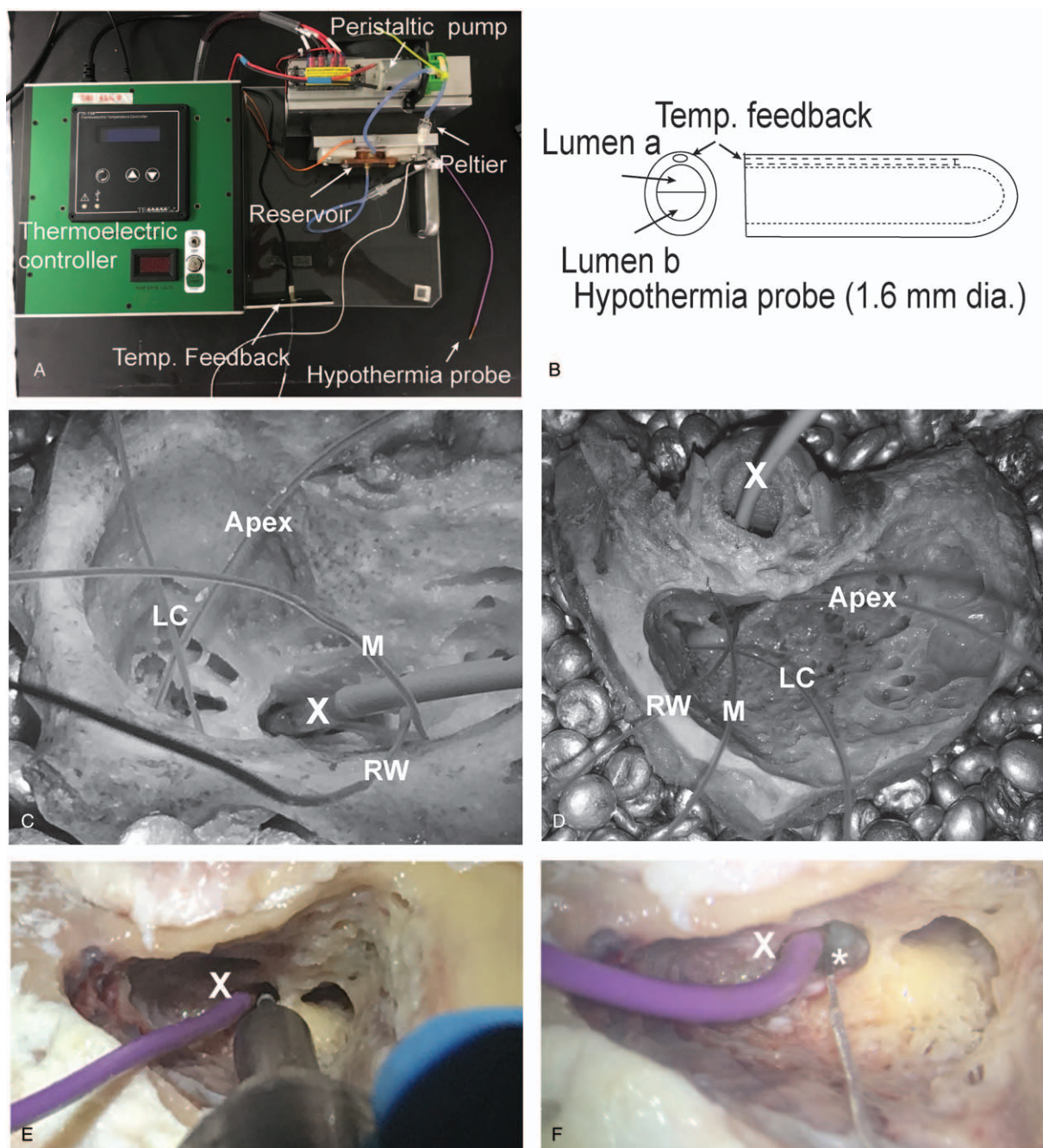
FIG. 3. Hypothermia system and experimental hypothermia setting. A custom-designed Peltier based thermoelectric system (*A*) and probe (*B*) were used to deliver therapeutic hypothermia to the temporal bones. A commercial thermoelectric controller drives Peltier system in contact with a reservoir filled with fluorocarbon. Temperature-controlled fluorocarbon is driven using a peristaltic pump into a multi-lumen tubing that ends in the hypothermia probe (*B*). Temperature feedback (target probe temperature) is obtained using a microthermistor placed in-line with probe lumen. Four other microthermistors are placed inside the RW (Apex), at RW annulus, over the lateral semicircular canal (LC) outer surface, and over the superior edge of the mastoidectomy (M) for the facial recess (*C*) and myringotomy (*D*) cooling approaches, respectively. With the hypothermia probe (X) in place, feasibility of bone drilling (*E*) and electrode placement (*F*, dummy implant marked with an *asterisk*) is demonstrated.

are depicted in Figure 4 for both approaches. Absolute temperatures measured every 2 minutes are shown in Figure 4A and C and change from baseline (at the initiation of cooling protocol) are shown in Figure 4B and D. With the facial recess approach, temperature at the round window reduced to 30 to 32 °C (a change of 5−7 °C from baseline), while that at the mastoid remained steady within ±0.5 °C of baseline. The myringotomy approach was similarly effective reducing temperature at the round window to 32.5 to 33 °C (a change of 3.5−4.3 °C from

TABLE 1. *Summary of μCT measurements means and range*

Measurement (Units)	Mean	Range
Distance between FN and ChT		
MID (mm)	0.91	0.4–1.5
IC (mm)	1.39	0.9–2.5
RW (mm)	2.59	1.5–3.3
SUP (mm)	2.86	2–4.3
Vertical plane measurements		
OR/MID and MID/IC (mm)	1.83	0.54–3.06
IC/RW (mm)	3.99	0.54–5.71
RW/SUP (mm)	0.96	0–3.88
FR HEIGHT (mm)	8.62	4.83–11.15
FR AREA (mm^2)	13.87	8.44–24.28
EAC ANGLE (°)	18.75	8.59–35.7
FN LOCATION (mm)		1.3 to −1.74[a]

ChT indicates chorda tympani; EAC ANGLE, angle between a line passing through the bony-cartilagineous junction of the EAC and the tympanic ring, and a line passing through the center of the basal turn of cochlea and through the antero-inferior aspect of the RW (Fig. 1D); FN LOCATION, distance between the anterolateral edge of the nerve and a line perpendicular to the basal turn line (Fig. 1F); FN, facial nerve; FR AREA, calculated facial recess area using fragmentation of total area as depicted by Figure 2; FR HEIGHT, total vertical span of the facial recess; IC, distance at inferior aspect of the EAC (Fig. 1A); IC/RW, vertical distance between IC μCT slice and slice depicting RW point; MID, distance at midpoint between chorda tympani origin and inferior aspect of the external auditory canal (EAC); MID/IC, vertical distance between MID μCT slice and slice depicting IC point; OR/MID, vertical distance between μCT slice with ChT origin and slice depicting MID point; RW, distance at the round window (Fig. 1B); RW/SUP, distance between RW μCT slice and slice depicting SUP point; SUP, distance at the superior-most μCT slice where ChT is still visible within its bony canal (before exiting behind the tympanic ring) (Fig. 1C).
[a]A negative value in this measurement represents a basal turn line that courses behind the anterolateral edge of the FN. All distances measured in mm, except for α angle (°).

baseline). The temperature at the lateral canal reduced by 2 to 2.8 °C with both the approaches. The temperature

profiles were highly consistent for the three repeated cycles.

Mean decreases in temperature from baseline and s.e.m. for all samples (n = 10, three repetitions per bone for a total of 30 measurements), recorded during the hypothermia protocol are summarized for RW, Apex, M, and LC in Figure 5 for the facial recess approach, and in Figure 6 for the myringotomy approach. Temperature values at four measurement points, at the beginning of the experiments (T_0) varied between 34.2 and 37.8 °C. The mean maximum decrease in temperature achieved in the experiments using the facial recess approach was 4.49 ± 1.68 °C for RW, 3.38 ± 1.12 °C for Apex, 2.36 ± 0.51 °C for LC, and 1.77 ± 0.72 °C for M, respectively. Cooling through a myringotomy approach produced a mean maximum decrease of 4.07 ± 0.98 °C for RW, 3.17 ± 0.95 °C for Apex, 2.6 ± 0.76 °C for LC and 1.87 ± 0.66 °C for M. There was no statistical difference in cooling efficiency, either for the maximum temperature change achieved at all four sites or the rate of cooling between the two different approaches. In FR approach, it took 9.4 ± 7.98 minutes to reduce the RW temperature by at least 2 °C. The time course was similar for the myringotomy approach: 9.33 ± 5.88 minutes ($p = 0.97$). Correlation analysis was conducted between radiologic measurements and both the maximum cooling and rate of cooling. The change of RW temperature, when the hypothermia was achieved via the FR, correlated with the EAC angle ($r = 0.44$, $p = 0.036$). However, the same was not true for the myringotomy approach ($r = 0.0414$, $p = 0.745$). Remaining factors, FR area or FN location revealed no significant correlation for the experimental measurements in either approach. The correlation coefficient between FR area and change at RW temperature was 0.041 ($p = 0.575$) and 0.017 ($p = 0.721$) and between FN location and change at RW temperature was 0.008 ($p = 0.272$) and 0.15 ($p = 0.806$) for FR and myringotomy approaches, respectively.

TABLE 2. *Summary of St. Thomas's Hospital (STH) classification grading and interventions for each bone*

Sample	L/R	STH Pre-	Intervention	STH Post- With Probe in FR/TM	EAC Angle (°C)	FR Area (mm^2)
1	L	2b	Independent cochleostomy	1/1	9.16	9.40
2	L	1	Membranous cochleostomy	1/1	35.7	12.29
3	L	1	Membranous cochleostomy	1/1	18.33	8.44
4	R	1	Membranous cochleostomy	1/1	20.3	12.66
5	R	1	Membranous cochleostomy	1/1	13.82	22.04
6	L	1	Membranous cochleostomy	1/1	34.39	10.67
7	R	1	Membranous cochleostomy	1/1	12.66	16.32
8	L	2a	Extended RW cochleostomy	1/1	17.88	24.28
9	R	2b	Independent cochleostomy	1/1	16.64	14.16
10	L	2b	Extended RW cochleostomy	1/1	8.59	8.48

Summary of visual grading for the temporal bones based on the STH classification. Column L/R depicts the laterality of the specimen. STH Pre- indicates the classification given to each bone upon wide opening of the facial recess and removal of any bony overhang on the RW niche to improve visualization. The column titled ''STH Post- with Probe in FR/TM'' indicates the new STH grading given to the visualization of the RW, extended RW, or independent cochleostomy, depending on intervention required for optimal exposure, together with the hypothermia probe in position through the facial recess or tympanic membrane. Individually calculated EAC angles and facial recess areas for each bone appear on the two right columns.
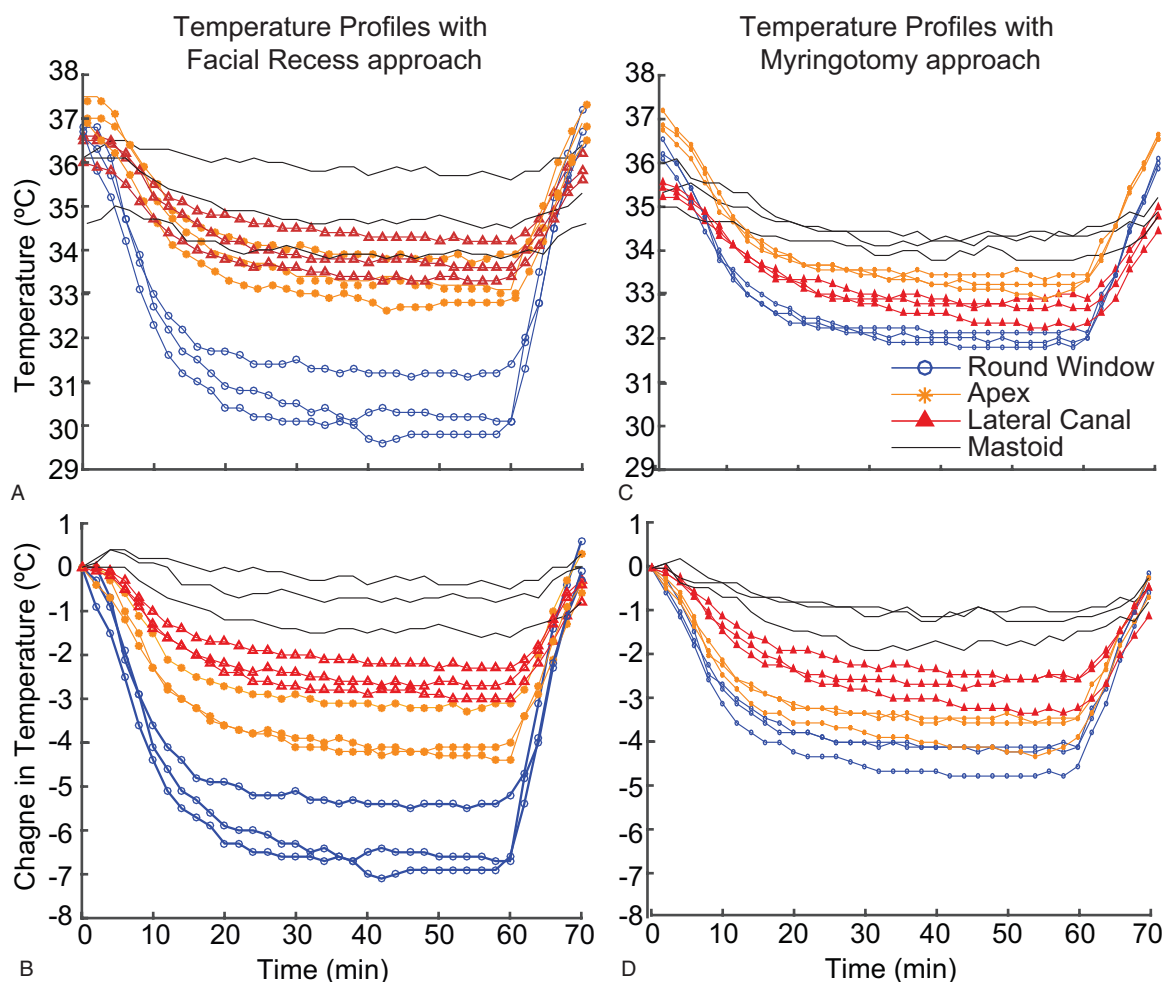
FIG. 4. Cooling profile for a single bone over time, in three consecutive hypothermia protocols, for both facial recess (*A* and *B*) and myringotomy (*C* and *D*) approaches. Absolute temperature is shown in *A* and *C* and change from baseline in *B* and *D*.

DISCUSSION

Mild therapeutic hypothermia applied between 32° and 34 °C is known to reduce oxidative stress associated with inflammatory cascades (35,36,44–46). Animal studies and clinical trials have provided evidence of therapeutic efficacy of hypothermia for seizures, stroke, cardiac arrest, and neurological trauma (39,46–58). Mechanistic molecular and epigenetic studies have demonstrated the potential for temperature to regulate immediate and delayed neuro-inflammatory responses impacting brain–blood barrier permeability, leukocyte recruitment, and programmed cell-death pathways. Initially studied in the setting of noise-induced ototoxicity (59), hypothermia's role in mitigating injury to the cochlea secondary to electrode insertion trauma is also now a validated concept (35,44).

The timing and method of hypothermia treatment plays a critical role in its therapeutic efficacy. Clinical trials on traumatic brain injury (TBI) and stroke have revealed that early initiation of therapeutic hypothermia following an acute insult results in improved functional outcomes (60,61). Equally important is the rate of rewarming post-hypothermia (62,63). Moreover, preclinical studies have shown that pre-traumatic hypothermia is neuro-protective and induces upregulation of molecular pathways that prevent cell death (61,64). Unfortunately, systemic hypothermia can lead to a number of side effects including immunosuppression, infection risk, insulin resistance, electrolyte disorders (60,65,66). However, locally administered therapeutic hypothermia enhanced neuroprotective benefits with little to no adverse effects in TBI and spinal cord injury (55,67). We have developed and validated the efficacy of a probe-based system for local delivery of therapeutic hypothermia to the cochlea (Fig. 3, (35,36)). Cochlear temperatures could be effectively reduced by 4 to 6 °C and maintained within ±0.3 °C, exemplifying the strict temperature control afforded by our technique. The approach also allows for controlled, slow rewarming. The current experiments demonstrate the ability of this technique to cool and sustain a stable hypothermic temperature in the human cochleae in simulated operating room conditions.
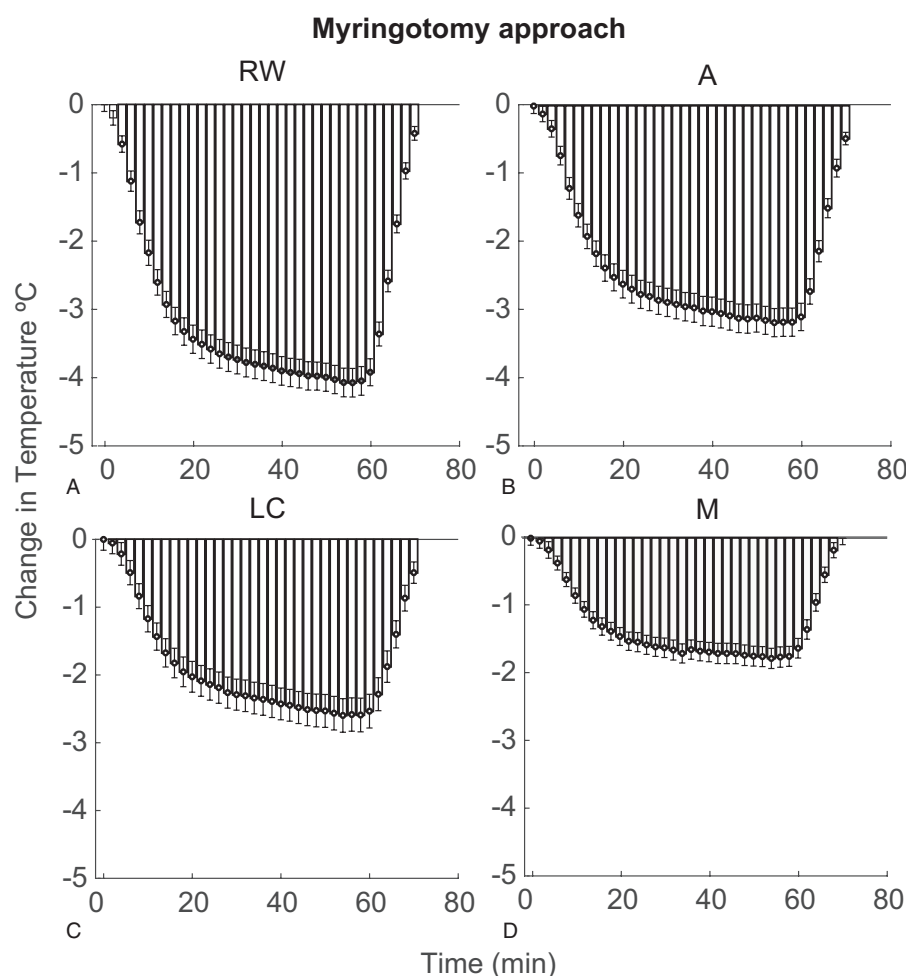
Facial Recess approach
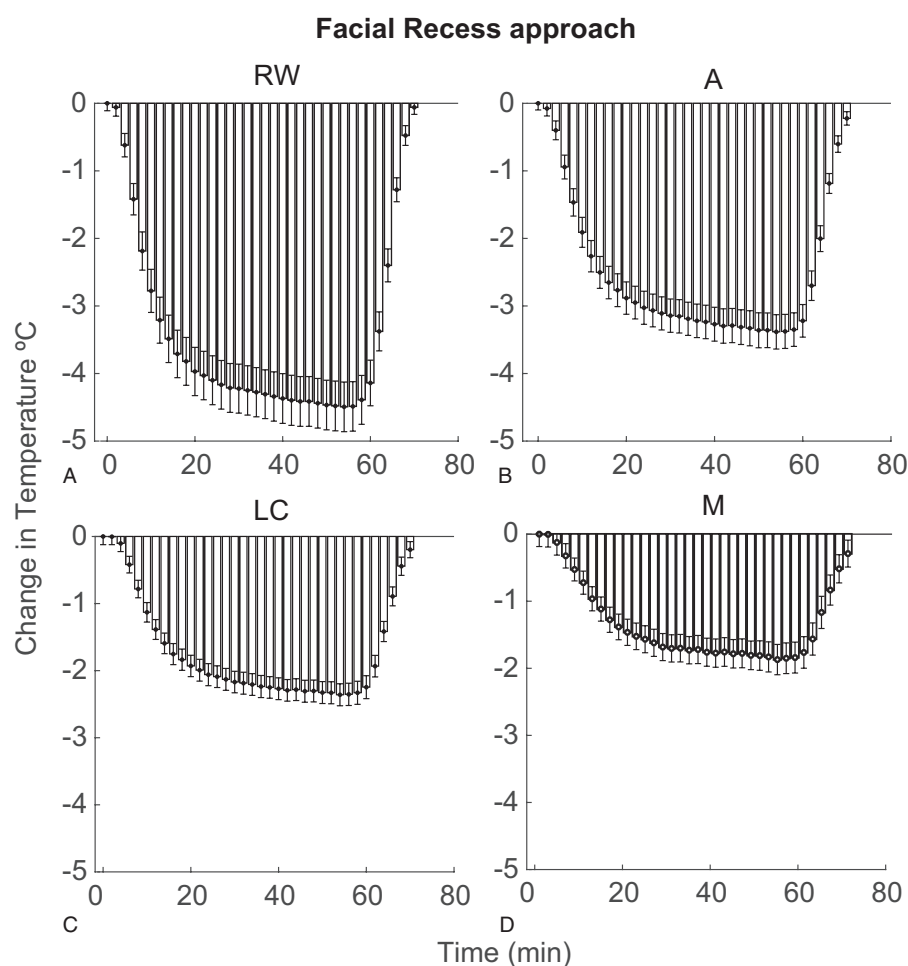
FIG. 5.   Means and standard errors for temperature change from baseline for all bones (n = 10, 30, total experiments), at sequential time points for RW (*A*), Apex (*B*), LC (*C*), and M (*D*) by the facial recess approach. LC indicates lateral semicircular canal; RW, round window.

The present study further analyzed the feasibility of using this technique in a clinical setting, considering the physical constraints of the human anatomy. In a clinical setting, a surgeon should be able to position and secure the cooling probe onto the cochlear promontory through the facial recess, allowing early initiation of cooling while preserving visualization of the RW for CI array insertion (Fig. 3C and D). An alternative approach would be to insert the cooling probe through a myringotomy. Either approach should permit ease of any promontory drilling required to complete a cochleostomy as well as electrode insertion while allowing cochlear hypothermia delivery. As denoted by the STH Post-grading (Table 2), excellent visualization for array insertion was conserved following positioning of the cooling probe through both approaches and optimization of the RW-, extended RW-, or independent cochleostomy-exposure. Moreover, temperature measurements demonstrated consistent hypothermia profiles, change in temperature and rate of cooling with our approach (Figs. 5 and 6). The myringotomy approach offered no added value to the local hypothermia treatment achieved with the more favorable

facial recess approach. Nevertheless, it serves as an effective alternative in cases where FR may be too contracted for appropriate visualization and insertion of hypothermia probe. This approach may also allow for initialization of cooling intraoperatively while mastoid bony work is being performed but with the added risk of a persistent tympanic membrane perforation in the context of a CI.

Several studies have sought to establish radiologic measurements that can predict degree of visualization during a standard facial recess approach (42,68,69). Of particular interest are the total FR area, the EAC angle and FN location. In all 10 specimens used in this study, good surgical visibility was achieved even with the cooling probe in place regardless of initial classification (Table 2). We then determined whether the listed radiologic measurements could also serve as predictors of visibility with the probe technique as well as whether they could predict differences in results of cooling trials. The surgical view of an adequately drilled FR is often tangential to the posterior bony EAC wall. Hence the narrower the EAC angle, the theoretically easier it is to

Myringotomy approach

FIG. 6. Means and standard errors for temperature change from baseline for all bones (n = 10, 30, total experiments), at sequential time points for RW (*A*), Apex (*B*), LC (*C*), and M (*D*) by the myringotomy approach. LC indicates lateral semicircular canal; RW, round window.

visualize a RW positioned along the basal turn axis. Although it may not always be predictive of RW visibility (42), narrower EAC angles may also translate to easier vectors for array insertion. If it leads to inherently different positioning of the cooling probe on the promontory, it may impact local temperature distribution. Finally, the FN location, measured as the distance between the most anterolateral aspect of the nerve and the basal turn axis line, can also serve as a surrogate of RW visibility and degree of obstruction posed by the nerve.

There was no significant correlation between degree of RW visualization using STH and the radiologic measurements. However, we had a smaller sample size compared with a previous study involving 70 ears (42). Moreover, takeoff of the ChT can play a significant role in total recess area without necessarily affecting RW visualization. Interestingly, we observed that there were no significant correlations between variability in facial recess areas or FN locations when compared with variability in the cooling parameters (maximum cooling and rate of cooling). EAC angle was correlated to maximum cooling

in facial recess approach but not in the myringotomy approach. This important finding suggests that such a technique can consistently achieve appropriate hypothermia treatment, locally, despite variability in temporal bone anatomy (Table 1).

In the current study, an appreciable change in temperature at the most distant thermistor positioned near the mastoid tip was observed, which may reflect limitations inherent to performing experiments on a cadaveric bone and a different positioning of the thermistor compared with previous study. Further, natural blood perfusion would likely prevent any significant changes in temperature to tissues not immediately adjacent to the cooling probe. Finally, the durations necessary for effective therapeutic cochlear hypothermia in a human undergoing CI implantation cannot be directly deduced from this study but must be extrapolated from preclinical models (35).

With evolving CI candidacy criteria that favor patients with significant residual hearing, our probe-based system for delivering local, mild therapeutic hypothermia to the inner ear for preservation of residual hearing can be a

critical component of the armamentarium for CI surgery. Our findings and approach can also be extended to pediatric CI, where preservation of residual hearing may greatly aid early language development and speech perception (5,70).

REFERENCES

1. FDA. FDA executive summary: premarket to postmarket shifts in clinical data requirements for cochlear implant device approvals in pediatric patients. Ear, Nose, and Throat Devices Panel of the Medical Devices Advisory Committee; 2015. Available at: https://wayback.archive-it.org/7993/20170114060413/http://www.fda.gov/downloads/AdvisoryCommittees/CommitteesMeetingMaterials/MedicalDevices/MedicalDevicesAdvisoryCommittee/EarNoseandThroatDevicesPanel/UCM443996.pdf. Accessed June 27, 2019.
2. Cochlear. Cochlear Annual Report 2016. Available at: http://www.cochlear.com/wps/wcm/connect/ebe550d5-d6c2-4b06-a1d2-8f873fb0c345/en_corporate_annualreport2016_2.37mb.pdf?MOD=AJPERES&CONVERT_TO=url&CACHEID=ROOT-WORKSPACE-ebe550d5-d6c2-4b06-a1d2-8f873fb0c345-lpSVNkn. 2016. Accessed June 27, 2019.
3. Hassepass F, Bulla S, Maier W, et al. The new mid-scala electrode array: a radiologic and histologic study in human temporal bones. *Otol Neurotol* 2014;35:1415–20.
4. Wanna GB, Noble JH, Carlson ML, et al. Impact of electrode design and surgical approach on scalar location and cochlear implant outcomes. *Laryngoscope* 2014;124 (suppl):S1–7.
5. Tobey EA, Thal D, Niparko JK, et al. Influence of implantation age on school-age language performance in pediatric cochlear implant users. *Int J Audiol* 2013;52:219–29.
6. Dorman MF, Gifford RH, Spahr AJ, et al. The benefits of combining acoustic and electric stimulation for the recognition of speech, voice and melodies. *Audiol Neurootol* 2008;13:105–12.
7. Gfeller KE, Olszewski C, Turner C, et al. Music perception with cochlear implants and residual hearing. *Audiol Neurootol* 2006;11 (suppl):12–5.
8. Gifford RH, Dorman MF, Skarzynski H, et al. Cochlear implantation with hearing preservation yields significant benefit for speech recognition in complex listening environments. *Ear Hear* 2013; 34:413–25.
9. Kang SY, Colesa DJ, Swiderski DL, et al. Effects of hearing preservation on psychophysical responses to cochlear implant stimulation. *J Assoc Res Otolaryngol* 2010;11:245–65.
10. Turner CW, Gantz BJ, Vidal C, et al. Speech recognition in noise for cochlear implant listeners: benefits of residual acoustic hearing. *J Acoust Soc Am* 2004;115:1729–35.
11. Rebscher SJ, Hetherington A, Bonham B, et al. Considerations for the design of future cochlear implant electrode arrays: electrode array stiffness, size and depth of insertion. *J Rehabil Res Dev* 2008;45:731–48.
12. Wright CG, Roland PS. Vascular trauma during cochlear implantation: a contributor to residual hearing loss? *Otol Neurotol* 2013;34:402–7.
13. Tanaka C, Nguyen-Huynh A, Loera K, et al. Factors associated with hearing loss in a normal-hearing guinea pig model of Hybrid cochlear implants. *Hear Res* 2014;316:82–93.
14. Wardrop P, Whinney D, Rebscher SJ, et al. A temporal bone study of insertion trauma and intracochlear position of cochlear implant electrodes. I: Comparison of Nucleus banded and Nucleus Contour electrodes. *Hear Res* 2005;203:54–67.
15. Bas E, Dinh CT, Garnham C, et al. Conservation of hearing and protection of hair cells in cochlear implant patients' with residual hearing. *Anat Rec (Hoboken)* 2012;295:1909–27.
16. Eshraghi AA, Polak M, He J, et al. Pattern of hearing loss in a rat model of cochlear implantation trauma. *Otol Neurotol* 2005;26: 442–7. discussion 7.
17. FDA. Executive Summary, Cochlear Corporation Nucleus Hybrid L24 System Premarket Approval P130016. Ear, Nose, and Throat Devices Panel of the Medical Devices Advisory Committee; 2013. Available at: https://www.fda.gov/downloads/AdvisoryCommittees/CommitteesMeetingMaterials/MedicalDevices/MedicalDevicesAdvisoryCommittee/EarNoseandThroatDevicesPanel/UCM373792.pdf. Accessed June 27, 2019.
18. Gantz BJ, Hansen MR, Turner CW, et al. Hybrid 10 clinical trial: preliminary results. *Audiol Neurootol* 2009;14 (suppl):32–8.
19. Kopelovich JC, Reiss LA, Etler CP, et al. Hearing loss after activation of hearing preservation cochlear implants might be related to afferent cochlear innervation injury. *Otol Neurotol* 2015;36:1035–44.
20. Prentiss S, Sykes K, Staecker H. Partial deafness cochlear implantation at the University of Kansas: techniques and outcomes. *J Am Acad Audiol* 2010;21:197–203.
21. Santa Maria PL, Domville-Lewis C, Sucher CM, et al. Hearing preservation surgery for cochlear implantation–hearing and quality of life after 2 years. *Otol Neurotol* 2013;34:526–31.
22. Koka K, Litvak LM. Feasibility of using electrocochleography for objective estimation of electro-acoustic interactions in cochlear implant recipients with residual hearing. *Front Neurosci* 2017;11:337.
23. Kontorinis G, Lenarz T, Stover T, et al. Impact of the insertion speed of cochlear implant electrodes on the insertion forces. *Otol Neurotol* 2011;32:565–70.
24. O'Connell BP, Holder JT, Dwyer RT, et al. Intra- and postoperative electrocochleography may be predictive of final electrode position and postoperative hearing preservation. *Front Neurosci* 2017; 11:291.
25. Rajan GP, Kontorinis G, Kuthubutheen J. The effects of insertion speed on inner ear function during cochlear implantation: a comparison study. *Audiol Neurootol* 2013;18:17–22.
26. Ramos BF, Tsuji RK, Bento RF, et al. Hearing preservation using topical dexamethasone alone and associated with hyaluronic acid in cochlear implantation. *Acta Otolaryngol* 2015;135:473–7.
27. Meshik X, Holden TA, Chole RA, et al. Optimal cochlear implant insertion vectors. *Otol Neurotol* 2010;31:58–63.
28. Ni Y, Dai P, Dai C, et al. Cochlear implant-related three-dimensional characteristics determined by micro-computed tomography reconstruction. *Clin Anat* 2017;30:39–43.
29. Astolfi L, Guaran V, Marchetti N, et al. Cochlear implants and drug delivery: in vitro evaluation of dexamethasone release. *J Biomed Mater Res B Appl Biomater* 2014;102:267–73.
30. Eshraghi AA, Adil E, He J, et al. Local dexamethasone therapy conserves hearing in an animal model of electrode insertion trauma-induced hearing loss. *Otol Neurotol* 2007;28:842–9.
31. James DP, Eastwood H, Richardson RT, et al. Effects of round window dexamethasone on residual hearing in a Guinea pig model of cochlear implantation. *Audiol Neurootol* 2008;13:86–96.
32. Scheper V, Hessler R, Hutten M, et al. Local inner ear application of dexamethasone in cochlear implant models is safe for auditory neurons and increases the neuroprotective effect of chronic electrical stimulation. *PLoS One* 2017;12:e0183820.
33. Stathopoulos D, Chambers S, Enke YL, et al. Development of a safe dexamethasone-eluting electrode array for cochlear implantation. *Cochlear Implants Int* 2014;15:254–63.
34. Van De Water TR, Abi Hachem RN, Dinh CT, et al. Conservation of hearing and protection of auditory hair cells against trauma-induced losses by local dexamethasone therapy: molecular and genetic mechanisms. *Cochlear Implants Int* 2010;11 (suppl): 42–55.
35. Tamames I, King C, Bas E, et al. A cool approach to reducing electrode-induced trauma: localized therapeutic hypothermia conserves residual hearing in cochlear implantation. *Hear Res* 2016;339:32–9.
36. Tamames I, King C, Huang CY, et al. Theoretical evaluation and experimental validation of localized therapeutic hypothermia application to preserve residual hearing after cochlear implantation. *Ear Hear* 2018;39:712–9.
37. Zhang H, Xu G, Zhang J, et al. Mild hypothermia reduces ischemic neuron death via altering the expression of p53 and bcl-2. *Neurol Res* 2010;32:384–9.

38. Darwazeh R, Yan Y. Mild hypothermia as a treatment for central nervous system injuries: positive or negative effects. *Neural Regen Res* 2013;8:2677–86.

39. Dietrich WD, Bramlett HM. The evidence for hypothermia as a neuroprotectant in traumatic brain injury. *Neurotherapeutics* 2010;7:43–50.

40. Takeda S, Hakuba N, Yoshida T, et al. Postischemic mild hypothermia alleviates hearing loss because of transient ischemia. *Neuroreport* 2008;19:1325–8.

41. Watanabe F, Koga K, Hakuba N, et al. Hypothermia prevents hearing loss and progressive hair cell loss after transient cochlear ischemia in gerbils. *Neuroscience* 2001;102:639–45.

42. Kashio A, Sakamoto T, Karino S, et al. Predicting round window niche visibility via the facial recess using high-resolution computed tomography. *Otol Neurotol* 2015;36:e18–23.

43. Leong AC, Jiang D, Agger A, et al. Evaluation of round window accessibility to cochlear implant insertion. *Eur Arch Otorhinolaryngol* 2013;270:1237–42.

44. Balkany TJ, Eshraghi AA, Jiao H, et al. Mild hypothermia protects auditory function during cochlear implant surgery. *Laryngoscope* 2005;115:1543–7.

45. Henry KR. Hyperthermia exacerbates and hypothermia protects from noise-induced threshold elevation of the cochlear nerve envelope response in the C57BL/6J mouse. *Hear Res* 2003;179:88–96.

46. Shintani Y, Terao Y, Ohta H. Molecular mechanisms underlying hypothermia-induced neuroprotection. *Stroke Res Treat* 2010; 2011:809874.

47. Atkins CM, Truettner JS, Lotocki G, et al. Post-traumatic seizure susceptibility is attenuated by hypothermia therapy. *Eur J Neurosci* 2010;32:1912–20.

48. Cappuccino A, Bisson LJ, Carpenter B, et al. The use of systemic hypothermia for the treatment of an acute cervical spinal cord injury in a professional football player. *Spine (Phila Pa 1976)* 2010; 35:E57–62.

49. Dietrich WD, Bramlett HM. Hyperthermia and central nervous system injury. *Prog Brain Res* 2007;162:201–17.

50. Dietrich WD, Levi AD, Wang M, et al. Hypothermic treatment for acute spinal cord injury. *Neurotherapeutics* 2011;8:229–39.

51. Kurz M, Lyden P, Lundbye J, et al. Local to Systemic Use of Hypothermia. *Ther Hypothermia Temp Manag* 2018;8:4–8.

52. Levi AD, Casella G, Green BA, et al. Clinical outcomes using modest intravascular hypothermia after acute cervical spinal cord injury. *Neurosurgery* 2010;66:670–7.

53. Matsui T, Ishikawa T, Takeuchi H, et al. Mild hypothermia promotes pro-inflammatory cytokine production in monocytes. *J Neurosurg Anesthesiol* 2006;18:189–93.

54. Ohta H, Terao Y, Shintani Y, et al. Therapeutic time window of post-ischemic mild hypothermia and the gene expression associated with the neuroprotection in rat focal cerebral ischemia. *Neurosci Res* 2007;57:424–33.

55. Purdy PD, Novakovic RL, Giles BP, et al. Spinal cord hypothermia without systemic hypothermia. *AJNR Am J Neuroradiol* 2013;34:252–6.

56. Yanamoto H, Nagata I, Nakahara I, et al. Combination of intra-ischemic and postischemic hypothermia provides potent and persistent neuroprotection against temporary focal ischemia in rats. *Stroke* 1999;30:2720–6. discussion 6.

57. Yokobori S, Bullock R, Gajavelli S, et al. Preoperative-induced mild hypothermia attenuates neuronal damage in a rat subdural hematoma model. *Acta Neurochir Suppl* 2013;118:77–81.

58. Yokobori S, Frantzen J, Bullock R, et al. The use of hypothermia therapy in traumatic ischemic /reperfusional brain injury: review of the literatures. *Therap Hypothermia Temp Manag* 2011;1:185–92.

59. Drescher DG. Effect of temperature on cochlear responses during and after exposure to noise. *J Acoust Soc Am* 1976;59:401–7.

60. Ahmed AI, Bullock MR, Dietrich WD. Hypothermia in traumatic brain injury. *Neurosurg Clin N Am* 2016;27:489–97.

61. Clifton GL, Jiang JY, Lyeth BG, et al. Marked protection by moderate hypothermia after experimental traumatic brain injury. *J Cereb Blood Flow Metab* 1991;11:114–21.

62. Povlishock JT, Wei EP. Posthypothermic rewarming considerations following traumatic brain injury. *J Neurotrauma* 2009;26: 333–40.

63. Thompson HJ, Kirkness CJ, Mitchell PH. Hypothermia and rapid rewarming is associated with worse outcome following traumatic brain injury. *J Trauma Nurs* 2010;17:173–7.

64. Lotocki G, de Rivero Vaccari JP, Perez ER, et al. Therapeutic hypothermia modulates TNFR1 signaling in the traumatized brain via early transient activation of the JNK pathway and suppression of XIAP cleavage. *Eur J Neurosci* 2006;24:2283–90.

65. Gebauer CM, Knuepfer M, Robel-Tillig E, et al. Hemodynamics among neonates with hypoxic-ischemic encephalopathy during whole-body hypothermia and passive rewarming. *Pediatrics* 2006;117:843–50.

66. Polderman KH. Mechanisms of action, physiological effects, and complications of hypothermia. *Crit Care Med* 2009;37:S186–202.

67. Tzen YT, Brienza DM, Karg PE, et al. Effectiveness of local cooling for enhancing tissue ischemia tolerance in people with spinal cord injury. *J Spinal Cord Med* 2013;36:357–64.

68. Lee DH, Kim JK, Seo JH, et al. Anatomic limitations of posterior tympanotomy: what is the major radiologic determinant for the view field through posterior tympanotomy? *J Craniofac Surg* 2012;23:817–20.

69. Teszler CB, Ruimi D, Bar-Meir E, et al. Width of the extended facial recess: a numerical study of ultrahigh-resolution computed tomography and its implications in minimally invasive otologic surgery. *Otol Neurotol* 2005;26:782–9.

70. Nikolopoulos TP, O'Donoghue GM, Archbold S. Age at implantation: its importance in pediatric cochlear implantation. *Laryngoscope* 1999;109:595–9.